On the Redox Reactions of Radicals with Al^{III}(phthalocyaninate) Pendants Covalently Bonded to Poly(ethyleneamide). Mechanistic Alterations When Radicals are Formed Inside Pockets of Micelle-Like Polymer Aggregates

G. T. Ruiz,[1] A. G. Lappin,[2] G. Ferraudi[3]

[1]Instituto de Investigaciones Fisicoquímicas Teóricas y Aplicadas (INIFTA, UNLP, CCT La Plata-CONICET), Diag. 113 y 64, Sucursal 4, C.C. 16, (B1906ZAA) La Plata, Argentina

[2]Department of Chemistry and Biochemistry, University of Notre Dame, Notre Dame, IN 46556

[3]Radiation Research Building, Department of Chemistry and Biochemistry, University of Notre Dame, Notre Dame, Indiana 46556-0579

Correspondence to: G. Ferraudi (E-mail: ferraudi.1@nd.edu)

ABSTRACT: The mechanisms of the redox reactions between a polymer containing Al(III) sulfonated phthalocyanine pendants, $(Al^{III}(^{\lfloor}NHS(O_2)trspc)^{2-})_2$, and radicals have been investigated in this work. Pulse radiolysis and photochemical methods were used for these studies. Oxidizing radicals, OH$^{\bullet}$, HCO$_3^{\bullet}$, (CH$_3$)$_2$COHCH$_2^{\bullet}$, and N$_3^{\bullet}$, as well as reducing radicals, e$_{aq}^{-}$, CO$_2^{\bullet-}$, and (CH$_3$)$_2$C$^{\bullet}$OH, respectively accept or donate one electron forming pendent phthalocyanine radicals, Al^{III}($^{\lfloor}$NHS(O$_2$)trspc $^{\bullet}$)$^{-}$ ^{or} $^{3-}$. The kinetics of the redox processes is consistent with a mechanism where the pendants react with radicals formed inside aggregates of five to six polymer strands. Electron donating radicals, that is, CO$_2^{\bullet-}$ and (CH$_3$)$_2$C$^{\bullet}$OH, produce one-electron reduced phthalocyanine pendants that, even though they were stable under anaerobic conditions, donated charge to a Pt catalyst. While the polymer was regenerated in the Pt catalyzed processes, 2-propanol and CO$_2$ were respectively reduced to propane and CO. The reaction of SO$_3^{\bullet-}$ radicals with the polymer stood in contrast with the reactions of the radicals mentioned above. A first step of the mechanism, the coordination of the SO$_3^{\bullet-}$ radical to the Al(III), was subsequently followed by the formation of a SO$_3^{\bullet-}$-phthalocyanine ligand adduct. The decay of the SO$_3^{\bullet-}$-phthalocyanine ligand adduct in a $\sim 10^2$ ms time domain regenerates the polymer, and it was attributed to the dimerization/disproportionation of SO$_3^{\bullet-}$ radicals escaping from the aggregates of polymer. © 2012 Wiley Periodicals, Inc. J Polym Sci Part A: Polym Chem 50: 2507–2515, 2012

KEYWORDS: catalysts; charge transfer; inorganic materials; macrocycles; metal-polymer complexes

INTRODUCTION Current interest in metal-free and metallo-phthalocyanines remains high because of their extensive applications to numerous fields of chemistry and biochemistry.[1–11] For example, the phthalocyanine of Al(III) and its derivatives have been used in various roles, which include being photosensitizers in photodynamic therapies.[8–10,12,13] Phthalocyanines incorporated in organic polymers, and polymerized phthalocyanines have been used as catalysts of reactions in the homogenous and heterogenous phase.[14,15] Moreover, the covalent binding of transition metal phthalocyanines as well as other transition metal complexes[7,11,16] have been used as a tool to change their physical and chemical properties. The covalent binding of the Al(III) phthalocyanine tetrasulfonate as pendants in a poly(ethyleneamide), (I) in Scheme 1, and the effect of such incorporation on the photophysical and photochemical properties of the phthalocyanine have been recently communicated.[17] Morphological studies of the polymer, poly(HOAl^{III}tspc), in aqueous solutions revealed that the strands of the polymer are associated in near spherical bundles with $\sim$ 150-diameter, Scheme 1. In these spherules, most of the pendants, represented here by the monomers Al^{III}($^{\lfloor}$NHS(O$_2$)trspc)$^{2-}$, (II), are forming π-stacks where the largest fraction of them must be dimers represented by $(Al^{III}(^{\lfloor}NHS(O_2)trspc)^{2-})_2$, (III).[17] It was also shown in this flash photolysis study of the polymer photochemistry that pendent radicals, Al^{III}($^{\lfloor}$NHS(O$_2$)trspc $^{\bullet}$)$^{-}$ and Al^{III}($^{\lfloor}$NHS(O$_2$)trspc $^{\bullet}$)$^{3-}$ were generated and that they reacted with scavengers trapped in the polymer pockets. Secondary radicals from the scavengers reactions escaped to the bulk of the solution where they catalyzed redox processes. These processes were observed in a 0.15- to 100-μs time domain. Because of the formation of spherules, solutions of the polymer are inhomogenous in nature with the material highly concentrated in the spherules. Differences of reactivity are expected when reactants, that is, inorganic and organic radicals, are
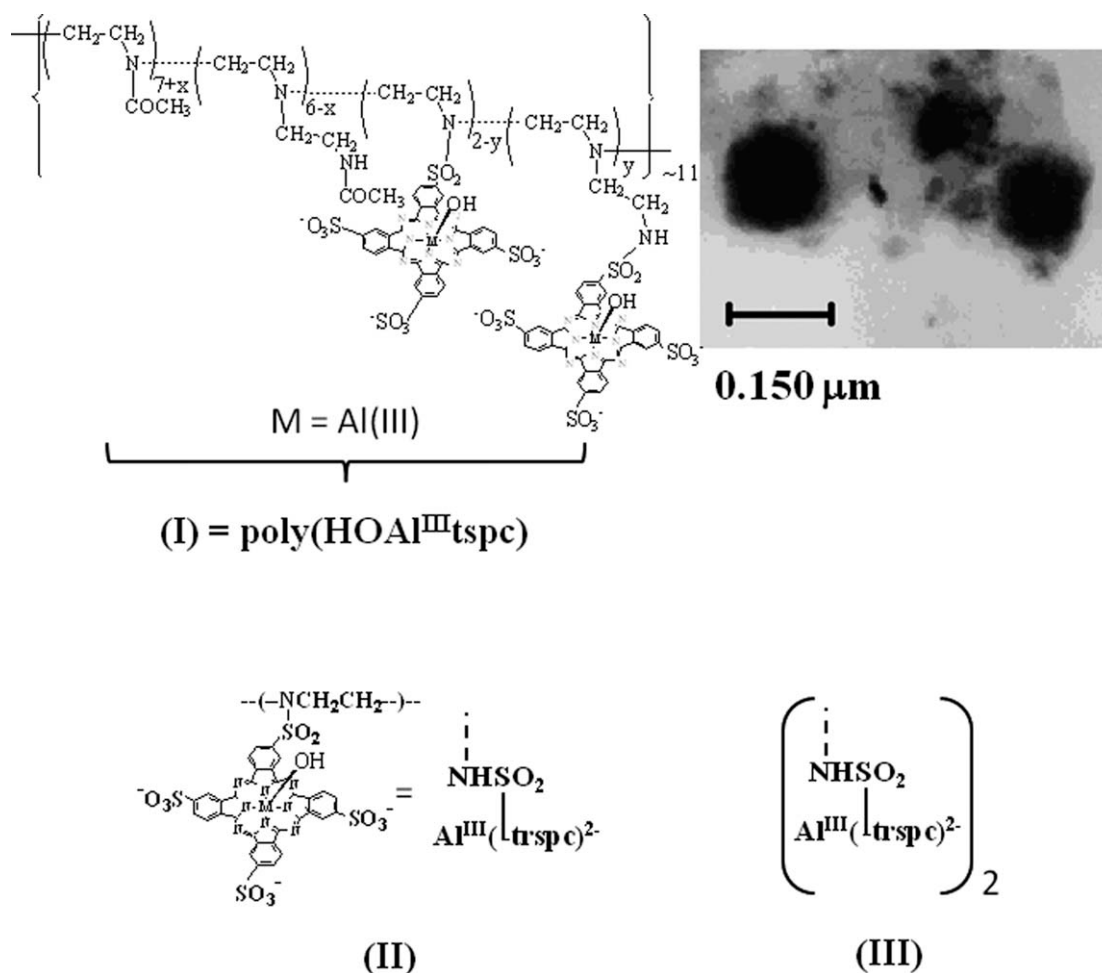
SCHEME 1 The polymer containing Al(III) sulfonated phthalocyanine, (I), is given the abbreviated name poly(HOAl^{III}tspc) in the text. A TEM picture of the polymer spherical aggregates is shown in the right side of the poly(HOAl^{III}tspc) structure. [17] The structure of the monomeric phthalocyanine pendant, (II), is abbreviated Al^{III}($^{\downarrow}$NHS(O$_2$)trspc)$^{2-}$ in the text where trspc stands for phthalocyaninetrisulfonate. The dimerized pendant, abbreviated as (Al^{III}($^{\downarrow}$NHS(O$_2$)trspc)$^{2-}$)$_2$, is shown in (III).

photochemically or thermally created. This work aims to broaden our knowledge of the generation and reactions of the pendant radicals. It is also a goal to study the mechanism of their redox reactions and explore potential applications in homogenous catalysis. Pulse radiolysis was the technique used for the kinetic and time-resolved spectroscopic studies. Steady state photochemical techniques were also used for an indirect generation of the radicals.

EXPERIMENTAL

Materials

The sodium salt of the tetrasulphonated Al(III) phthalocyanine, Na$_3$[Al^{III}tspc], and poly(HOAl^{III}tspc), repeating unit C$_{134}$H$_{160}$N$_{38}$O$_{30}$S$_8$Al$_2$Na$_6$ with MW = 3.2 × 10^3, were available from a previous work and used without further purifications. [17] Buffers in the poly(HOAl^{III}tspc) and Na$_3$[Al^{III}tspc] solutions used for the experiments were pH = 10, prepared with reagent grade Fisher's 0.05 M buffer solution pH = 10 and pH = 6–7 buffers prepared with NaH$_2$PO$_4$ and Na$_3$PO$_4$. Ultra high purity N$_2$ and N$_2$O were used for the deaeration of the solutions.

Pulse-Radiolytic Procedures

Pulse radiolysis experiments were carried out with a model TB-8/16-1S electron linear accelerator following previously described methods. [7,18] The instrument and computerized data collection for time-resolved UV-Vis spectroscopy, and reaction kinetics have been described elsewhere in the literature. [19] Thiocyanate dosimetry was carried out at the beginning of each experimental session. The details of the dosimetry have been reported elsewhere. [19,20] The procedure is based on the concentration of (SCN)$_2^{\bullet-}$ radicals generated by the electron pulse in a N$_2$O saturated 10^{-2} M SCN$^-$ solution. In the procedure, the calculations were made with $G = 6.13$ and an extinction coefficient, $\varepsilon = 7.58 \times 10^3$ M^{-1}·cm^{-1} at 472 nm, for the (SCN)$_2^{\bullet-}$ radicals. [19,20] In general, the experiments were carried out with doses that in N$_2$ saturated aqueous solutions resulted in (2.0 ± 0.1) × 10^{-6} M to (6.0 ± 0.3) × 10^{-6} M concentrations of e$^-_{aq}$. In these experiments, solutions were deaerated with streams of the O$_2$-free gas, N$_2$ or N$_2$O, that was required for the experiment. In N$_2$O-saturated solutions, reactions of the radiolytically generated OH$^{\bullet}$ radicals with N$_3^-$, SO$_3^{2-}$, methanol, 2-propanol, and

radiolytic pulse

$+ N_2O, + H^+$
$- N_2$ ⤳ $OH^\bullet \cdots$ → OH^-

$X^- \xrightarrow{\quad\quad} X^\bullet$

$X^- = HCO_2^-, SO_4^{2-}, N_3^-, CH_3OH, (CH_3)_3COH$;

$X^\bullet = CO_2^{\bullet-}, SO_4^{\bullet-}, N_3^\bullet, C^\bullet H_2OH, (CH_3)_2COHC^\bullet H_2$
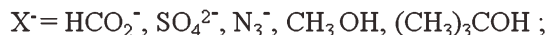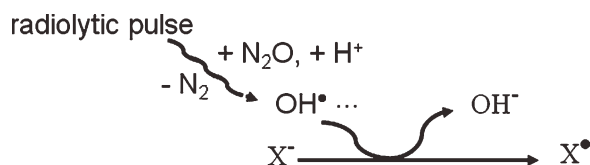
SCHEME 2 Radiolytic generation of radicals by $OH^\bullet$.

2-methyl-2-propanol were used for the preparation of reactive radicals, for example, $N_3^\bullet$, $CO_2^{\bullet-}$, $HCO_3^\bullet$, $SO_3^{\bullet-}$, $C^\bullet H_2OH$, $(CH_3)_2C^\bullet OH$ and $(CH_3)_2COHC^\bullet H_2$, Scheme 2.

Other experiments, where the simultaneous generation of $(CH_3)_2COHC^\bullet H_2$ and e_{aq}^- was desired, were conducted with N_2-deaerated solutions containing 0.1 M $(CH_3)_3COH$ as a scavenger of the radiolytically generated $OH^\bullet$ radicals.

To radiolyze a fresh sample with each radiolytic pulse, an appropriate flow of the solution through the reaction cell was maintained during the experiment. When the radiolyzed solutions had a pH = 10, the radicals $C^\bullet H_2O^-$ and $C^\bullet H_2OH$ radicals were produced in a molar relationship 1:5. This mixture of the $C^\bullet H_2O^-$ and $C^\bullet H_2OH$ radicals produced at pH = 10 will be generically described as $C^\bullet H_2OH$ radicals in the following sections. Other conditions used for the time-resolved spectroscopy of the reaction intermediates or in the investigation of the reaction kinetics are given in the Results section.

The reaction kinetics was investigated by following the absorbance change at given wavelengths of the spectrum and incorporating those changes in the dimensionless parameter, $\xi = (\Delta A_{inf} - \Delta A_t)/(\Delta A_{inf} - \Delta A_0)$.[21] In ξ, ΔA_0 is the absorbance change at the beginning of the reaction, ΔA_t is determined at an instant t of the reaction and ΔA_{inf} is determined at the end of the reaction.

Photochemical Procedures

Aqueous solutions of poly(HOAl^{III}tspc) containing 3.0 M $(CH_3)_2CO$ and 3.0 M $(CH_3)_2CHOH$ were deaerated for half an hour with streams of N_2 in a gas tight cell. They were irradiated with 300-nm light, $I_0 \sim 10^{-4}$ Einstein L^{-1} min^{-1}, from a Rayonet lamp after the deaeration was completed. The concentrations of poly(HOAl^{III}tspc), indicated in the Results section, used in these experiments so that 99.99% of the light was absorbed by $(CH_3)_2CO$. To analyze the photochemically produced propane by GC chromatography, the photolyzed solutions were first frozen to $N_2(l)$ temperature. The N_2-deaerated suspension of the Pt catalyst was added by the syringe procedure without loss of gas on top of the frozen solution. After the mixture was thawed and the reaction complete, the liquid was brought to $N_2(l)$ temperature. Non-condensable products were transferred using vacuum line techniques to a GC-17A Shimadzu chromatograph. A molecu-

lar sieves column, RT-Q-Plot, and a TC detector were used for the separation and detection of the products.

Photolysis of poly(HOAl^{III}tspc) in N_2-deaerated aqueous solutions containing 0.12-M triethanolamine,TEOA, was carried out with polychromatic light, $\lambda > 500$ nm. Only the $Al^{III}(^\llcorner NHS(O_2)trspc)^{2-}$ chromophores absorbed the 500-nm light under this conditions. A variation of the procedure used for the analysis of propane was followed for the production and analysis of CO. The cell containing the photolyzed solution was purged with ultrahigh purity CO_2 before it was frozen to $N_2(l)$ temperature. The subsequent addition of the Pt catalyst and the handling of the frozen mixture was done as indicated above for the propane analysis.

RESULTS

Oxidation and Reduction of Pendants by Radicals

The reactions of the phthalocyanine pendants with oxidizing radicals, $R_{ox}^\bullet = OH^\bullet$, $HCO_3^\bullet$, $(CH_3)_2COHCH_2^\bullet$ and $N_3^\bullet$, and reducing radicals, $R_{red}^\bullet = e_{aq}^-$, $CO_2^{\bullet-}$ and $(CH_3)_2C^\bullet OH$, were investigated by pulse radiolysis. The same spectrum (Fig. 1) was produced when $HCO_3^\bullet$, $(CH_3)_2COHCH_2^\bullet$ and $N_3^\bullet$ radicals react with the phthalocyanine pendants. Because $HCO_3^\bullet$ and $N_3^\bullet$ radicals are typically electron acceptors and no reactions with groups in the polymer strand can be expected, the product of the reaction was assigned as the phthalocyanine
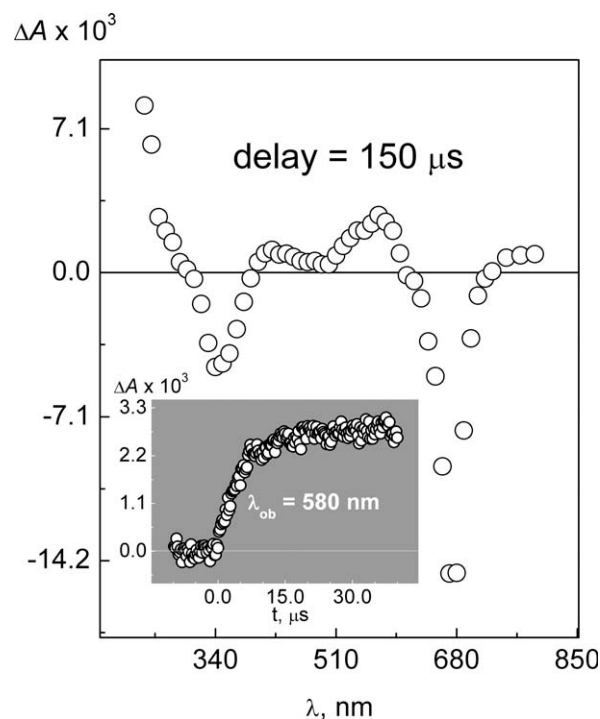
FIGURE 1 Typical difference spectrum recorded when radicals oxidize $Al^{III}(^\llcorner NHS(O_2)trspc)^{2-}$ pendants. The spectrum was recorded 150 μs after the radiolytic generation of $HCO_3^\bullet$ radicals in a solution containing 1.4×10^{-5} M pendants at pH = 10. An oscillographic trace in the inset shows the growth of the $Al^{III}(^\llcorner NHS(O_2)trspc \bullet)^-$ absorbance at 580 nm.
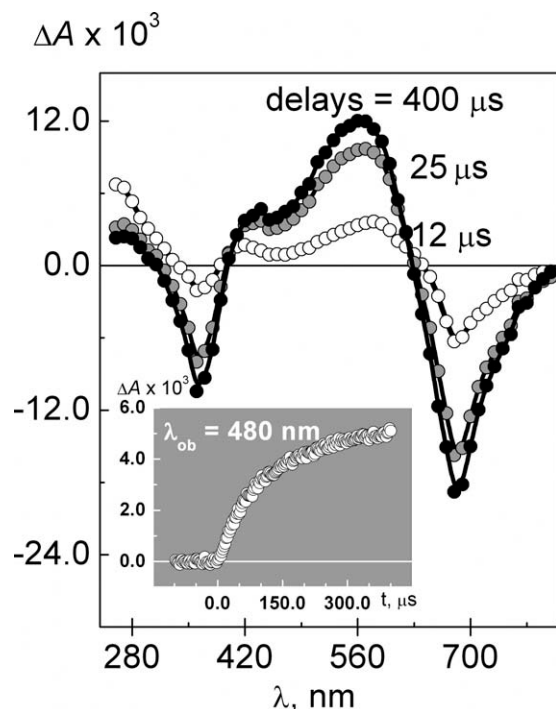
FIGURE 2 Typical difference spectra recorded when radicals reduce $Al^{III}(^{\llcorner}NHS(O_2)trspc)^{2-}$ pendants. The spectra was recorded with different delays after the radiolytic generation of $(CH_3)_2C^\bullet OH$ radicals in a solution containing 1.1×10^{-5} M pendants at pH = 10. An oscillographic trace in the inset shows the growth of the $Al^{III}(^{\llcorner}NHS(O_2)trspc^\bullet)^{3-}$ absorbance at 480 nm.

radical, $Al^{III}(^{\llcorner}NHS(O_2)trspc^\bullet)^-$, produced by the one electron oxidation of the polymer pendants, eq 1.

$$\left(\begin{matrix} | \\ NHSO_2 \\ Al^{III}(^{\llcorner}trspc)^{2-} \end{matrix} \right)_2 + R_{ox}^\bullet \longrightarrow \left(\begin{matrix} | & | \\ NHSO_2 & NHSO_2 \\ Al^{III}(^{\llcorner}trspc^\bullet)^- & Al^{III}(^{\llcorner}trspc)^{2-} \end{matrix} \right) + R_{ox}^- \quad (1)$$
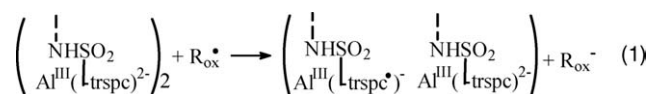
Consistent with the assignment of the spectrum in Figure 1 to $Al^{III}(^{\llcorner}NHS(O_2)trspc^\bullet)^-$ pendants are the similarity of the spectrum with the literature spectrum of the $Al^{III}(tspc^\bullet)^{3-}$.[12,13,17] With a similar reasoning, the spectra produced when $CO_2^{\bullet-}$ and $(CH_3)_2C^\bullet OH$ radicals react with the phthalocyanine pendants (Fig. 2) correspond to the phthalocyanine radical, $Al^{III}(^{\llcorner}NHS(O_2)trspc\bullet)^{3-}$, produced by the one-electron reduction of the macrocycle, eq 2.

$$\left(\begin{matrix} | \\ NHSO_2 \\ Al^{III}(^{\llcorner}trspc)^{2-} \end{matrix} \right)_2 + R_{red}^\bullet \longrightarrow \left(\begin{matrix} | & | \\ NHSO_2 & NHSO_2 \\ Al^{III}(^{\llcorner}trspc^\bullet)^{3-} & Al^{III}(^{\llcorner}trspc)^{2-} \end{matrix} \right) + R_{red}^+ \quad (2)$$
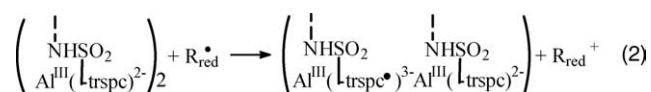
Oscillographic traces following the spectroscopic changes caused by the reactions of the polymer with $CO_2^{\bullet-}$, $(CH_3)_2C^\bullet OH$, $HCO_3^\bullet$, and $N_3^\bullet$ radicals were recorded at particu-

lar wavelengths of the spectra, that is, where the bleach of the solutions and the appearance of new absorption bands were positioned. All the traces were fitted to biexponentials, $1-(A_1 \exp(-k_1 t) + A_2 \exp(-k_2 t))$, where k_1 varies between 6×10^5 and 3×10^4 s^{-1} and k_2 varies between 8×10^4 and 3×10^3 s^{-1}. Rate constants for the formation of oxidized and reduced pendant radicals are given in Table 1.[22,23]

The reduction of poly(HOAl^{III}tspc) by e_{aq}^- was carried out in a solution containing 1.3×10^{-5} M $Al^{III}(^{\llcorner}NHS(O_2)trspc)^{2-}$ pendants and 0.01 M $(CH_3)_3COH$. It exhibited a faster kinetics than the reactions of the previously mentioned radicals and took place in parallel with a reaction between the pendants and $(CH_3)_2COHCH_2^\bullet$ radicals. Indeed, the spectrum recorded with delays equal to or shorter than 20 μs from the radiolysis pulse was a convolution of the spectra of the $Al^{III}(^{\llcorner}NHS(O_2)trspc^\bullet)^-$ and $Al^{III}(^{\llcorner}NHS(O_2)trspc^\bullet)^{3-}$ chromophores. Oscillographic traces recorded at given wavelengths between 700 and 400 nm were well fitted to biexponentials, $1-(A_1 \exp(-k_1 t) + A_2 \exp(-k_2 t))$ (Table 1). A comparison between the rate constants respectively calculated for the e_{aq}^- reaction and the $(CH_3)_2COHCH_2^\bullet$ reaction with the polymer shows that they have similar values. On the basis of these rate constants, it is not surprising that the transient spectrum generated in the e_{aq}^- reaction with poly(HOAl^{III}tspc) and $(CH_3)_3COH$ as the scavenger $OH^\bullet$ radicals is a convolution of the spectra of the $Al^{III}(^{\llcorner}NHS(O_2)trspc^\bullet)^-$ and $Al^{III}(^{\llcorner}NHS(O_2)trspc^\bullet)^{3-}$ chromophores. The overall process is schematically represented by eqs 3 and 4 where the curly arrow shows only the formation of the e_{aq}^- and $OH^\bullet$ radicals by the radiolysis of the solution.
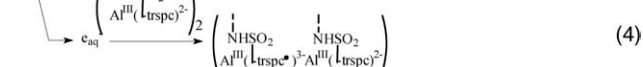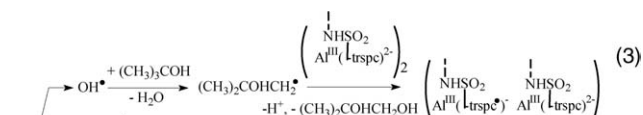
The reaction of $OH^\bullet$ radicals with poly(HOAl^{III}tspc) was investigated in a N_2O saturated solution containing 1.3×10^{-5} M $Al^{III}(^{\llcorner}NHS(O_2)trspc)^{2-}$ pendants. In contrast to the reactions of the e_{aq}^- and $(CH_3)_2COHCH_2^\bullet$ with poly(HOAl^{III}tspc), the reaction of the $OH^\bullet$ radicals occurs in a fast single step. Oscillographic traces showing the formation of the product were fitted to a exponential, $1-\exp(-t/\tau_1)$ where $\tau_1 = 3.6$ μs. The spectra recorded with delays equal to or longer than 10 μs, that is, after the formation of the $OH^\bullet$ radicals, are almost identical to the spectra generated with the oxidizing radicals $HCO_3^\bullet$, $(CH_3)_2COHCH_2^\bullet$ and $N_3^\bullet$. It must be assigned therefore to the generation of $Al^{III}(^{\llcorner}NHS(O_2)trspc^\bullet)^-$ pendants in the reaction of poly(HOAl^{III}tspc) with $OH^\bullet$ radicals. Some spectral differences with the spectrum of the $Al^{III}(^{\llcorner}NHS(O_2)trspc^\bullet)^-$ pendants were observed at wavelengths shorter than 350 nm in a $t < 10$ μs time scale. They must be attributed to other radicals formed

TABLE 1 Rate Constants for the Reactions Between Radicals and $Al^{III}(^{\downarrow}NHS(O_2)trspc\,)^{2-}$ Pendants and the Reduction Potential of Radical Couples

Radical	$k_1/10^5\ s^{-1}$	$k_2/10^3\ s^{-1}$	k_1/k_2	$[Al^{III}(^{\downarrow}NHS(O_2)trspc\,)^{2-}]$ $\times 10^5$, M[a]	Reduction Potentials, V[b]
					$R_{ox}{}^{\bullet}/R_{ox}{}^{-}$
$OH^{\bullet}$	2.8	–		1.3	2.8
$N_3^{\bullet}$	1.2	30	4.0	1.4	1.7[c]
$HCO_3^{\bullet}$	0.11	2.6	4.2	1.4[d]	2.1
$(CH_3)_2COHCH_2^{\bullet}$	6.1	134	4.6	1.3	0.6
					$R_{red}{}^{+}/R_{red}{}^{\bullet}$
e_{aq}^{-}	7.2	120	6	1.3	−2.75
$CO_2^{\bullet-}$	0.54	9.3	5.8	1.9	−1.2
$(CH_3)_2C^{\bullet}OH$	0.27	4.2	6.4	1.1	−1.2

[a] Concentration of pendant in the solution used in the experiment. Solutions buffered at pH =10 unless stated.
[b] Values from Ref. 22.
[c] Revised value in Ref. 23
[d] Solutions with pH = 7 used in these experiments.

when the $OH^{\bullet}$ reacts with groups, for example, amide, in the polymer backbone. Such radicals account for a minor and slower oxidation in the period between 10 and a 100 μs producing more $Al^{III}(^{\downarrow}NHS(O_2)trspc^{\bullet})^{-}$ pendants.

The Compounded Reaction of the $SO_3^{\bullet-}$ Radicals

In contrast to the $OH^{\bullet}$ radical, the $SO_3^{\bullet-}$ radical is a moderate oxidant with some tendency to add to aromatic double bonds. It was the only radical generated in these experiments by the oxidation of a dianion, that is, 0.1 M SO_3^{2-} at pH = 9.5. Spectra recorded in a time scale $t < 1\ \mu s$ coincide with the literature spectrum of the $SO_3^{\bullet-}$ radical.[24] A spectrum, different of those assigned above to $Al^{III}(^{\downarrow}NHS(O_2)trspc^{\bullet})^{-}$ and $Al^{III}(^{\downarrow}NHS(O_2)trspc^{\bullet})^{3-}$ pendent radicals, grew in a time domain 1 $\mu s < t \leq$ 1ms (Fig. 3). Contrary to expectations based on the spectra of the $Al^{III}(^{\downarrow}NH-S(O_2)trspc^{\bullet})^{-}$ and $Al^{III}(^{\downarrow}NHS(O_2)trspc^{\bullet})^{3-}$ chromophores, no absorption bands appear in the 400–600 nm spectroscopic region, no intense bleach of the Q-band is observed at $\sim$700 nm and an uncharacteristic absorption band appears at $\sim$680 nm. A similar spectrum was observed when pulse radiolytically generated $SO_3^{\bullet-}$ radicals reacted with 1 × 10^{-4} M $Al^{III}(tspc)^{3-}$ at pH = 9.5 demonstrating that other groups present in the polymer strand had no effect on the course of the reaction. The long-lived intermediate was tentatively assigned as a $SO_3^{\bullet-}$-phthalocyanine ligand adduct. For reasons presented in the Discussion and a comparison with a similar product formed in the reaction between $SO_3^{\bullet-}$ and $Al^{III}(tspc)^{3-}$, the adduct must be a radical different of the $Al^{III}(^{\downarrow}NHS(O_2)trspc^{\bullet})^{-}$ and $Al^{III}(^{\downarrow}NHS(O_2)trspc^{\bullet})^{3-}$.

The reaction of the polymer with pulse radiolytically generated $SO_3^{\bullet-}$ radicals is a biphasic process. Oscillographic traces recorded for the reaction of $SO_3^{\bullet-}$ radicals with the polymer at different wavelengths of the spectrum, that is, 350, 420, 575, and 675 nm, were all fitted to a biexponential, $1 - w_1 \exp(-t/\tau_1) + w_2 \exp(-t/\tau_2))$ where $\tau_1 = 150\ \mu s$ and $\tau_2 = 1.7$ ms. The biexponential behavior with highly dis-

similar τ_1 and τ_2 lifetimes is a feature of a mechanism involving two sequential processes each with a first or pseudo-first order kinetics, eq 5.

$$\left(\begin{array}{c}^{|}_{NHSO_2}\\ Al^{III}(^{\downarrow}_{trspc})^{2-}\end{array}\right)_2 + SO_3^{\bullet-} \xrightarrow{\tau_1} \begin{array}{c}\text{Short - lived}\\ \text{Intermediate}\end{array} \xrightarrow{\tau_2} \begin{array}{c}\text{Long - lived}\\ \text{Intermediate}\end{array} \quad (5)$$
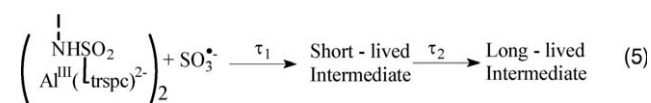
The reactions of 1.0 × 10^{-4} M and 4.0 × 10^{-4} M $Al^{III}(tspc)^{3-}$ with $SO_3^{\bullet-}$ radicals occurs also in two steps and the oscillographic traces can be fitted to a biexponential
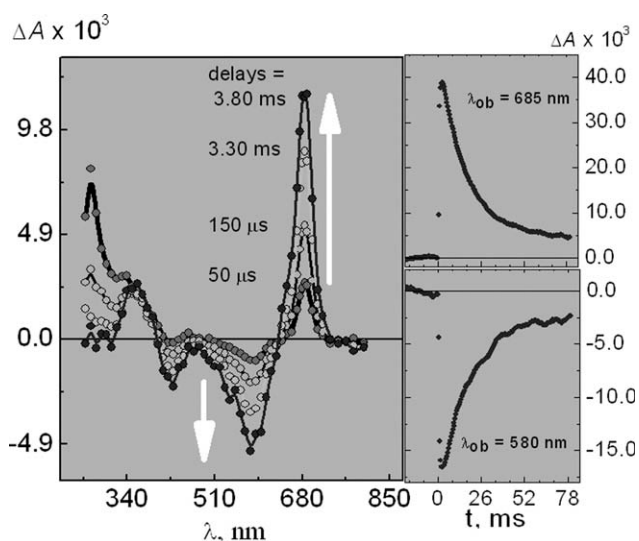
FIGURE 3 Transient difference spectra (left) observed when $SO_3^{\bullet-}$ radicals react with $Al^{III}(^{\downarrow}NHS(O_2)trspc)^{2-}$. The spectra was recorded with different delays after the radiolytic generation of $SO_3^{\bullet-}$ radicals in a 0.1 M SO_3^{2-} solution buffered at pH = 9.5 containing also 1.1× 10^{-5} M pendants. Arrows indicate the sense of the change with time. Traces (right) recorded respectively at λ_{ob} = 580 and 685 nm show the decay of the long lived transient in a much longer time scale.

$1 - (A_1 \exp(-k_1 t) + A_2 \exp(-k_2 t))$ with a pseudo-first order rate constant $k_1 = 1.5 \times 10^6$ s^{-1} and a first order rate constant 2.0×10^4 s^{-1}. A second order rate constant, $k = 1.5 \times 10^{10}$ M^{-1} s^{-1} was calculated dividing the pseudo-first order rate constant by the concentration of Al^{III}(tspc)$^{3-}$. Transient spectra recorded during the first step of the process bear no resemblance with the spectrum of Al^{III}(tspc$^\bullet$)$^{2-}$ and/or Al^{III}(tspc$^\bullet$)$^{4-}$. Coordination of the SO$_3^{\bullet-}$ radical to the Al(III) with the corresponding small changes in the absorption spectrum of the phthalocyanine chromophore provides a better rationale of the spectroscopic changes. In addition, the diffusion controlled rate of this step, while being acceptable for a coordination reaction, is too fast relative to the known rates of the SO$_3^{\bullet-}$ radical redox and addition reactions. The position and intensity of the changes in the spectrum during the second step of the process are consistent with the formation of a SO$_3^{\bullet-}$-phthalocyanine adduct with a rate constant 2.0×10^4 s^{-1}.

To investigate the fate of the long-lived intermediate, eq 5, a solution of the composition indicated above was irradiated with 40 radiolysis pulses and the UV-Vis spectrum compared with the spectrum of a nonirradiated blank. Since the spectra of the solution recorded before and after irradiation showed no differences, it was concluded that the decay of the long-lived intermediate returns the polymer to its initial condition. The decay of the long-lived intermediate was followed at wavelengths of the transient absorbance decay, $\lambda_{ob} = 350$ and 680 nm, and the recovery of the bleach, $\lambda_{ob} = 430$ and 570 nm. Fairly linear plots, ξ^{-1} versus time were obtained for 80% or more of the long-lived intermediate's decay followed at all the mentioned wavelengths. Ratios of the rate constant to the extinction coefficient calculated at these various wavelengths are: $2k/\varepsilon = 1.87 \times 10^3$ cm s^{-1} ($\Delta A_0 = 3.85 \times 10^{-2}$) at 685 nm, 3.54×10^3 cm s^{-1} ($\Delta A_0 = -1.66 \times 10^{-2}$) at 580 nm and 5.26×10^3 cm s^{-1} ($\Delta A_0 = 1.0 \times 10^{-2}$) at 340 nm. The slow decay of the long-lived intermediate contrasts with the fast decay of the radical produced in the experiment with Al^{III}(tspc)$^{3-}$. Indeed, a ratio of the rate constant to the extinction coefficient at $\lambda_{ob} = 340$ nm is $2k/\varepsilon = 7.3 \times 10^6$ cm s^{-1} ($\Delta A_0 = 1.0 \times 10^{-2}$) in the experiments with Al^{III}(tspc)$^{3-}$.

Stability of Al^{III}($^|$NHS(O$_2$)trspc$^\bullet$)$^{3-}$ Pendants

The observation of Al^{III}($^|$NHS(O$_2$)trspc$^\bullet$)$^{3-}$ pendants in pulse radiolysis was limited to a period $t < 2$ ms. To investigate the fate of the radical pendants over longer periods, they were generated photochemically using the 300-nm photolysis, $I_0 \sim 10^{-4}$ Einstein L^{-1} min^{-1}, of acetone in the presence of 2-propanol as a source of (CH$_3$)$_2$C$^\bullet$OH radicals, eqs 6 and 7.

$$(CH_3)_2CO \xrightarrow{+ h\nu\ (\lambda=300\ \text{nm}),\ \phi} {}^3(n\pi)(CH_3)_2CO \xrightarrow{(CH_3)_2CHOH} 2\ (CH_3)_2C^\bullet OH \quad (6)$$

$$\left(\underset{Al^{III}(^|_{trspc})^{2-}}{\overset{^|NHSO_2}{|}} \right)_2 + (CH_3)_2C^\bullet OH \longrightarrow \left(\underset{Al^{III}(^|_{trspc}^\bullet)^{3-}\cdot Al^{III}(^|_{trspc})^{2-}}{\overset{^|NHSO_2 \qquad ^|NHSO_2}{| \qquad\qquad |}} \right) + (CH_3)_2CO + H^+ \quad (7)$$
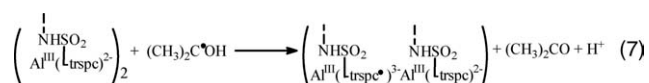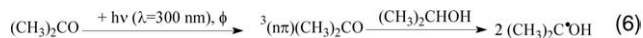
In this procedure, (CH$_3$)$_2$C$^\bullet$OH radicals were generated photolyzing deaerated aqueous solutions of the polymer containing 3.4 × 10^{-5} M or 1.3 × 10^{-4} M pendants, 3. M (CH$_3$)$_2$CO and 3. M (CH$_3$)$_2$CHOH. The solutions changed color from green to dark blue over a period of 2–3 min of irradiation and showed the characteristic spectrum of the Al^{III}($^|$NHS(O$_2$)trspc$^\bullet$)$^{3-}$ chromophore (Fig. 4). All the absorption bands positioned at $\lambda > 450$ nm disappear after a lengthier irradiation due to the hydrogenation of a double bond in the macrocycle forming the leuco phthalocyanine moiety. As it was previously communicated, no changes in the absorption spectrum were observed when a deaerated aqueous solution of the polymer containing 1.3 × 10^{-4} M pendants but not (CH$_3$)$_2$CO and (CH$_3$)$_2$CHOH was photolyzed at 300 nm.[17]

Under anaerobic conditions, both Al^{III}($^|$NHS(O$_2$)trspc$^\bullet$)$^{3-}$ and the leuco phthalocyanine pendants were kept in their respective solutions without change for more than 24 h. Conversely, Al^{III}($^|$NHS(O$_2$)trspc$^\bullet$)$^{3-}$ pendants in the 2-propanol–acetone mixed solvent were rapidly oxidized back to the Al^{III}($^|$NHS(O$_2$)trspc)$^{2-}$ pendants upon aeration of the solution. They were also quantitatively converted to the Al^{III}($^|$NHS(O$_2$)trspc)$^{2-}$ pendants when the Pt catalyst was added anaerobically to the photolyzed solution. The GC analysis of the gas produced after the conversion of the Al^{III}($^|$NHS(O$_2$)trspc$^\bullet$)$^{3-}$ to the Al^{III}($^|$NHS(O$_2$)trspc)$^{2-}$ pendants revealed the presence of propane. Oxidation of the leuco phthalocyanine pendants either by O$_2$ or by the solvent in the presence of the Pt catalyst to the original oxidation state

FIGURE 4 Spectra showing the formation of the Al^{III}($^|$NH-S(O$_2$)trspc $^\bullet$)$^{3-}$ radical pendants in the 300 nm photolysis, $I_0 \sim 10^{-4}$ Einstein L^{-1} min^{-1}, of 3.0 M acetone in the presence of 3.0 M 2-propanol as a source of (CH$_3$)$_2$C$^\bullet$OH. The dashed line corresponds to the formation of the leuco pendants after an extensive photolysis.

through processes that are slower than those of the $Al^{III}(^{\llcorner}NHS(O_2)trspc\ ^\bullet)^{3-}$ pendants.

$Al^{III}(^{\llcorner}NHS(O_2)trspc\ ^\bullet)^{3-}$ pendants were also generated by the $\lambda > 500$ nm photolysis of deaerated aqueous solution of the polymer containing 1.3×10^{-4} M $Al^{III}(^{\llcorner}NHS(O_2)trspc)^{2-}$ pendants and 0.12 M TEOA. When the Pt catalyst was added anaerobically to the solution of $Al^{III}(^{\llcorner}NHS(O_2)trspc\ ^\bullet)^{3-}$ pendants, they remained unaffected for a period longer than 24 h. but were oxidized slowly in the presence of the catalyst by CO_2. The GC analysis of the gas after the reaction with CO_2 was completed showed the formation of CO as a product.

$Al^{III}(tspc^\bullet)^{2-}$ radicals, were photochemically generated by the reduction of $2\ 10^{-4}$ M $Al^{III}(tspc)^{3-}$ with $(CH_3)_2C^\bullet OH$ radicals as indicated above for the preparation of the equivalent $Al^{III}(^{\llcorner}NHS(O_2)trspc\ ^\bullet)^{3-}$ pendants. Although the deep blue color of the $Al^{III}(tspc^\bullet)^{2-}$ is appreciable during the photolysis, it faded a few seconds after the photolysis was stopped. Over an exposure period of ~ 15 min to the 300-nm light, the solution acquired the yellow color of the leuco phthalocyanine. The rapid decay of the $Al^{III}(tspc^\bullet)^{4-}$ radicals occurs mainly via eq 8 where the $Al^{III}(tspcH_2)^{3-}$ product has an hydrogenated phthalocyanine ligand.

$$2\ Al^{III}(tspc^\bullet)^{4-} \xrightarrow[-\ 2\ HO^-]{+\ 2\ H_2O}\ Al^{III}(tspc)^{3-} + Al^{III}(tspcH_2)^{3-} \qquad (8)$$
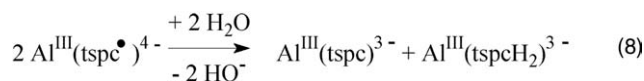
DISCUSSION

The reactions of the $Al^{III}(^{\llcorner}NHS(O_2)trspc)^{2-}$ pendants in the polymer are more diverse than those of the $Al^{III}(tspc)^{3-}$.[1-3] Such diversity can be associated with the inclusion of the $Al^{III}(^{\llcorner}NHS(O_2)trspc)^{2-}$ pendants in aggregates of many polymer strands and with the polyelectrolyte nature of the strands.[17] These are some structural and morphological features of poly(HOAl^{III}tspc) demonstrated in a previous work. Because of the aggregation of strands, there is a low concentration of aggregates in the poly(HOAl^{III}tspc) solutions and a very high concentration of pendants in the spherical aggregates. Estimates, shown below, yield a $\sim 4 \times 10^{-8}$ M average concentration of aggregates in a solution containing 1.0×10^{-5} M $Al^{III}(^{\llcorner}NHS(O_2)trspc)^{2-}$ pendants and an average of ~ 66 pendants per aggregate. As a consequence of the solution's heterogenous nature, rate constants greater than 4×10^4 s^{-1} yield second order rate constants in great excess of those reported in the literature for the reactions of the radicals investigated in this work. Moreover, some of the calculated rate constants reach values above the limit expected for a diffusion controlled reaction rate. Rate constants (Table 1) greater than 4×10^4 s^{-1} must be ascribed, therefore, to processes occurring within the aggregates. In this regard, the generation and reactions of the radicals within the poly (HOAl^{III}tspc) aggregates closely resemble similar processes of micelle-entrapped substrates.[25-27] Some other conditions inside the aggregates, for example, the medium conditions,

must affect the rate of the reactions between the $Al^{III}(^{\llcorner}NHS(O_2)trspc)^{2-}$ pendants and the radicals. Indeed, comparisons of the rate constants of the $CO_2^{\bullet-}$ and $(CH_3)_2C^\bullet OH$ reactions and $HCO_3^\bullet$ and $N_3^\bullet$ reactions do not show the expected dependence of the rate constant on the reduction potential of the radical (Table 1). Factors such as the mobility of the radical in the aggregates must have a significant bearing on the values of the rate constants.

The rate constants calculated for the $N_3^\bullet$ and $(CH_3)_2COHCH_2^\bullet$ reactions are in a $k_1/k_2 \sim 4$ relationship, whereas $k_1/k_2 \sim 6$ for the e_{aq}^-, $CO_2^{\bullet-}$ and $(CH_3)_2C^\bullet OH$ reactions (Table 1). Because these relationships between k_1 and k_2 are close to the proportions of dimeric to monomeric pendants in the aggregates, it can be argued that the fast step, that is, with rate constant k_1, corresponds to reactions of the radicals with the dimeric pendants. The slow step, that is, with rate constant k_2, will be then ascribed to the reaction of the radicals with the less abundant monomer pendants. Appropriate conditions must exist, for example, a correct relationship between k_1 and k_2, to observe a biexponential kinetics. Indeed, the reaction rate of the $HCO_3^\bullet$ radicals with the dimeric pendants could be sufficiently slow to distinguish it from the reaction of the radicals with the monomeric pendants. Also, reactions of the OH$^\bullet$ radical with other groups in poly(HOAl^{III}tspc) can rapidly deplete the concentration of OH$^\bullet$ radicals inside the aggregates for the second step to be observed.

Contrary to the reactions of the OH$^\bullet$ radical, no reaction of the $SO_3^{\bullet-}$ radical with groups in the polymeric backbone are expected. The first step can be regarded as the diffusion and reaction of the radiolytically generated $SO_3^{\bullet-}$ radicals with pendants inside the polymer aggregates. Coordination of the $SO_3^{\bullet-}$ radical to the Al(III), that is, replacing OH$^-$ and/or H_2O ligands, is a possible process consistent with the experimental observations. The process is similar to the one occurring in the first step of the reaction the $SO_3^{\bullet-}$ radical with $Al^{III}(tspc)^{3-}$. Coordination of the $SO_3^{\bullet-}$ radical to either Al(III) metal centers to form the short-lived intermediate, eq 5, will cause little changes in the absorption spectrum but it will affect the rate of formation of the long-lived intermediate. If the coordination of the $SO_3^{\bullet-}$ radical to the Al(III) metal center of $Al^{III}(^{\llcorner}NHS(O_2)trspc)^{2-}$ in the aggregates is as fast as in the $Al^{III}(tspc)^{3-}$ reaction, it is possible to make the approximation $150 \times 10^{-6} = 1/(k_d \times [\text{aggregates}])$ where $k_d \sim 2 \times 10^9$ M^{-1} s^{-1} is the diffusion rate constant and [aggregates] $\sim 3.3 \times 10^{-6}$ M is the aggregate's concentration. In this approximation, it is assumed that the *effective diffusion coefficient* of the $SO_3^{\bullet-}$ radical is not much different of the diffusion coefficient in solution. Namely, $\varepsilon_i\ \delta/\tau \sim 1$ where ε_i is *porosity* available for the transport, δ is the *constrictivity* and τ is the *tortuosity* inside the aggregate.[28] The diffusion rate constant $k_d \sim 2 \times 10^9$ M^{-1} s^{-1} was calculated on the basis of the Smoluchowski equation.[29,30] In the calculation, the diffusion coefficient of the aggregate, $D \le 10^{-11}$ m^2 s^{-1}, negligible with respect to the radical, $D \sim 1 \times 10^{-9}$ m^2 s^{-1}, the electrostatic interaction between charges in the aggregate and the anion radical and a ~ 75-nm radius of the
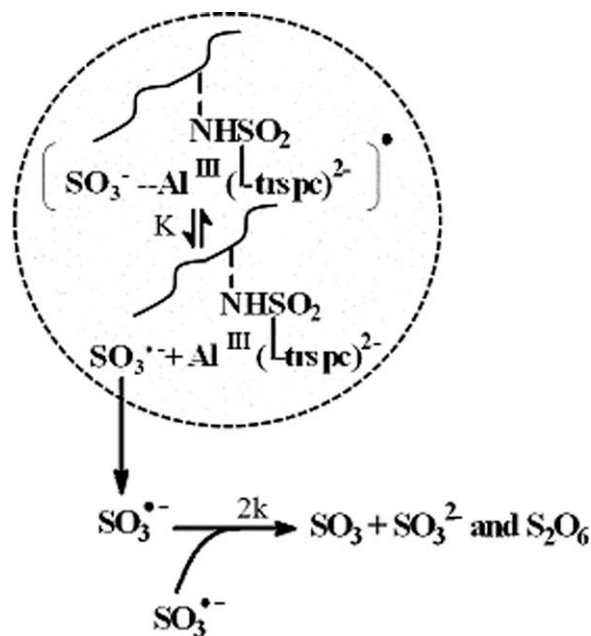
SCHEME 3 Proposed mechanism of the $SO_3^{\bullet-}$—phthalocyanine adduct decay. The aggregate is represented by the circle where K is an equilibrium constant for the dissociation of the adduct in its constituents. $SO_3^{\bullet-}$ radicals that escape from the aggregate undergo disproportionation and/or dimerization with an overall rate constant 2k. The disappearance of the adduct will be kinetically of a second order with an integrate rate law,[21] $-d[\rho_{adduct}]/dt = (2k\,K/\rho_{pendant}) \times [\rho_{adduct}]^2$, where ρ_{adduct} and $\rho_{pendant}$ are respectively the molar densities of adducts and pendants in the aggregate.

aggregate were considered. Since the estimated concentration of strands in the same solution is $\sim 1.8 \times 10^{-5}$ M, there must be an average of approximately five to six strands per aggregate. In the second step of the mechanism, eq 5, insertion of the $SO_3^{\bullet-}$ radical into the phthalocyanine macrocycle forms a phthalocyanine radical, that is, the long-lived intermediate. In some regards, the addition process bears a resemblance with the formation of an adduct in the reaction of the $SO_3^{\bullet-}$ radical with $Ni^{II}CR^+$.[18] Marked differences can be seen between the spectrum of the radical and the spectra of those formed in reactions where radicals function as electron donors, for example, e_{aq}^-, $CO_2^{\bullet-}$ and $(CH_3)_2C^{\bullet}OH$, or acceptors, for example, $HCO_3^{\bullet}$ and $N_3^{\bullet}$. They signal the structural differences existing between radicals produced by the one electron removal, eq 1, or addition, eq 2, to the phthalocyanine macrocycle and the radical formed by the addition of the $SO_3^{\bullet-}$ radical.

The decay of the $SO_3^{\bullet-}$ adduct to the phthalocyanine macrocycle, that is, the long-lived intermediate, is faster in $Al^{III}(tspc)^{3-}$, $2k/\varepsilon = 7.3 \times 10^6$ cm s^{-1}, than in the $Al^{III}(^{\downarrow}NHS(O_2)trspc)^{2-}$ pendants, $2k/\varepsilon \approx 2.6 \times 10^3$ cm s^{-1}. A $\sim 10^{-4}$ deceleration of the reaction in the polymer can be attributed to medium conditions inside the aggregates that provide a larger stability to the adduct between the $SO_3^{\bullet-}$ radical and the phthalocyanine ligand. The dissociation of

the adduct can also be kinetically arrested in pockets of the aggregate. This effect will be similar to molecular fragment, for example, a pair of radicals, trapped in the solvent cage or in pockets of a molecular sieve. Both, medium conditions and trapping inside the pockets of the aggregates, must have a retardation effect on the separation of the $SO_3^{\bullet-}$ radical from the macrocycle. Changes in the absorption spectrum associated with the decay of the $SO_3^{\bullet-}$-phthalocyanine ligand adduct show that $Al^{III}(^{\downarrow}NHS(O_2)trspc)^{2-}$ pendants are regenerated and the rate of the process exhibits an inverse dependence on the concentration of intermediate. A probable path for the decay involves the diffusion of $SO_3^{\bullet-}$ radicals out of the aggregates followed by the rapid radical—radical annihilation in the bulk of the solution, Scheme 3.

CONCLUSIONS

Reactions of radiolytically generated radicals with poly(HOA-l^{III}tspc) and micelle-entrapped substrates show some mechanistic similarities. Such similarities are most likely a consequence of the radicals being generated within loose aggregates of polymer strands. Because the phthalocyanine radicals generated in the polymer aggregates have lost mobility, their lifetimes are greatly augmented becoming pseudostable species. One can expect that pendent radicals will exhibit long lifetimes in the absence of solvolytic and/or unimolecular decomposition processes. This is being observed with the one electron reduced pendants, $Al^{III}(^{\downarrow}NHS(O_2)trspc^{\bullet})^{3-}$, but it is not the case with the unstable one electron oxidized $Al^{III}(^{\downarrow}NHS(O_2)trspc^{\bullet})^-$ pendant radical. For pendant radicals showing long lifetimes, some applications may result from such pseudostability. For example, the reduced polymer can be used as a storage of electronic charge and be incorporated later in a chemical process as it was done in the Pt-catalyzed respective reductions of 2-propanol to propane and CO_2 to CO.

REFERENCES AND NOTES

1 Leznoff, C. C.; Lever, A. B. P., Eds.; Phthalocyanines: Properties and Applications; VCH: New York, **1989,** 1993, 1996; Vols. *1–4.*

2 Lever, A. B. P. *J. Porphyrins Phthalocyanines* **2004,** *8*, 1327–1342.

3 Chen, J.; Lever, A. B. P. *J. Porphyrins Phthalocyanines* **2007,** *11*, 151–159.

4 Halma, M.; Castro, K. A. D. F.; Taviot-Gueho, C.; Prévot, V.; Foranoc, C.; Wypych, F.; Nakagaki, S. *J. Catal.* **2008,** *257*, 233–243.

5 Bohrer, F. I.; Colesniuc, C. N.; Park, J.; Schuller, I. K.; Kummel, A. C.; Trogler, W. C. *J. Am. Chem. Soc.* **2008,** *130*, 3712–3713.

6 Bedioui, F.; Griveau, S.; Nyokong, T.; Appleby, A. J.; Caro, C. A.; Gulppi, M.; Ochoae, G.; Zagal, J. H. *Phys. Chem. Chem. Phys.* **2007**, *9*, 3383–3396.

7 Thomas, S.; Ruiz, G.; Ferraudi, G.; *Macromolecules* **2006**, *39*, 6615–6621.

8 Rosenthal, I. In Developments in Photobiology of Phthalocyanines, Phthalocyanines: Properties and Applications; Leznoff, C. C.; Lever, A. B. P., Eds.; VCH: New York, **1996;** Vol. *4*, Chapter 13.

9 Kunz, L.; Connelly, J. P.; Woodhams, J. H.; MacRobert, A. J. *Photochem. Photobiol. Sci.* **2007**, *6*, 940–948.

10 Labanauskiene, J.; Gehl, J.; Didziapetriene, J. *Bioelectrochemistry* **2007**, *70*, 78–82.

11 Wöhrle, D.; Benters, R. O.; Suvorova, G.; Schnurpfeil, N.; Trombach Bogdahn-Rai, T. *J. Porphyrins Phthalocyanines* **2000**, *4*, 491–497.

12 Ferraudi, G.; Argüello, G. A.; Ali, H.; van Lier, J. E. *Photochem. Photobiol.* **1988**, *47*, 657–680.

13 Phillips, D. *Prog. React. Kinet.* **1997**, *22*, 175–380.

14 Brouwer, W. M.; Piett, P.; German, A. L. *J. Mol. Catal.* **1985,** *29*, 335–395.

15 Sivanesan, A.; John, S. A. *Electrochim. Acta* **2008**, *53*, 6629–6635.

16 Manners, I. *Science* **2001**, *294*, 1664–1666.

17 Ruiz, G. T.; Ferraudi, G.; Lappin, A. G. *J. Photochem. Photobiol. A: Chem.* **2009**, *206*, 1–9.

18 Dutta, S. K.; Ferraudi, G. *J. Phys. Chem. A* **2001**, *105*, 4241–4247.

19 Hug, G. L.; Wang, Y.; Schöneich, C.; Jiang, P.-Y.; Fessenden, R. W. *Radiat. Phys. Chem.* **1999**, *54*, 559–566.

20 Buxton, G. V.; Greenstock, C. L.; Hellman, W. P.; Ross, A. B. *J. Phys. Chem. Ref. Data* **1988,** *17*, 513–886.

21 Frost, A. A.; Pearson, R. G. In Kinetics and Mechanism;Wiley: New York, **1953;** Chapter 3, pp 28–31.

22 Wardman, P. *J. Phys. Chem. Ref. Data* **1989,** *18*, 1637–1755.

23 Ruiz, G. T.; Juliarena, M. P.; Wolcan, E.; Ferraudi, G. *Inorg. Chim. Acta* **2007,** *360*, 3681–3687.

24 Hayon, E. *J. Chem. Phys.* **1969,** *51*, 4881–4892.

25 Hubig, S. M.; Rodgers, M. A. J. *J. Phys. Chem.* **1990,** *94*, 1933–1936.

26 Roodt, A.; Sullivan, J. C.; Meisel, D.; Deutsch, E. *Inorg. Chem.* **1991,** *30*, 4545–4549.

27 Visser, A. J. W. G.; Fendler, J. H. *J. Phys. Chem.* **1982,** *86*, 947–950.

28 Grathwohl, P. In Diffusion in Natural Porous Media. Contaminant Transport, Sorption/Desorption and Dissolution Kinetics; Kluwer, Marcel Deker, New York, NY, **1998.**

29 Czerlinski, G. H. In Chemical Relaxation; Marcel Decker, **1966;** Chapter 12, pp 244–248,

30 Brogioli, D.; Vailati, A. *Phys. Rev. E.* **2001,** *63*, 12105-1–12105-4.